# Indium tin oxide single-mode waveguide modulator

Ray T. Chen, Dan Robinson, Huey Lu, Lev Sadovnik, and Zonh-Zen Ho

Physical Optics Corporation
2545 West 237th Street, Suite B
Torrance, California 90505

## ABSTRACT

We have successfully demonstrated an $In_2O_3$:Sn semiconductor thin film waveguide. The energy gap of the film can be manipulated from 3.1 eV (0.4 μm) to 3.7 eV (0.335 μm) by changing the ratio of $In_2O_3$ and $SnO_2$. Waveguide propagation losses of 3 dB/cm for transverse magnetic (TM) and 8 dB/cm for transverse electric (TE) guided waves were experimentally confirmed at the wavelength of 632.8 nm. A phase modulator containing an indium tin oxide waveguide, two holographic mirrors, two microprisms, and two ohmic contacts was fabricated. Electro-optic (current injection) and all optical modulations were conducted. A modulation depth of 18% was experimentally confirmed for the current injection device, using 15-volt applied voltage, and a modulation depth of 15% using 250 mW 355 nm UV light as the activation sources. An $In_2O_3$:Sn waveguide device working at the cutoff boundary was made. A modulation depth of 26 dB was measured with an applied voltage of 30 volts. An array of applications, including use in current sensors, ozone UV sensors, attenuated total reflection (ATR) modulators, delay lines for phased array antennae and multi-quantum wells are highly feasible.

## 1.0 INTRODUCTION

We report the development of a new $In_2O_3$ film for use as an optical waveguide and an electrooptic and all-optic modulator. The $In_2O_3$:Sn film has good transparency which allows a large number of optical wavelengths to be multiplexed with the carrier signal. The index of refraction of the $In_2O_3$:Sn film shifts from 2.0 with 100% $In_2O_3$ to 1.75 with 95% $In_2O_3$ and 5% $SnO_2$ at the 632.8 nm wavelength. Furthermore, the $In_2O_3$:Sn is a semiconductor film, so the effective index of the guided mode can be modulated by current injection.[1-3] With an electric field or an optical beam as the origin of the current injection, electrooptic (current injection) and all-optic modulators, respectively, can be made with the proposed thin film.

Film characteristics, such as transmission bandwidth, band gaps of $In_2O_3$:Sn films as a function of $In_2O_3$ concentrations, and carrier density, are described in Section 2.0. Theoretical and experimental work aimed at providing a single-mode waveguide are also reported in Section 2.0 where waveguiding characteristics and waveguide propagation losses for both TE and TM modes at wavelength of 0.6328 μm are described. The working principle of the active device for both electrooptic (current injection) and all-optic modulation is detailed in Section 3.0. The experimental results are further described in Section 4.0. A Fabry-Perot waveguide resonator was employed for intensity modulation. Further applications, including a short interaction length attenuated total reflection (ATR) waveguide modulator, a current sensor, a UV sensor, and a multi-quantum well (MQW) device are described in Section 5.0, followed by concluding remarks.

## 2.0 FORMATION OF AN $In_2O_3$:$S_n$ SEMICONDUCTOR THIN FILM WAVEGUIDE

Transparent, electrically conducting $In_2O_3$ films are widely used in solar energy conversion, in optoelectronics, and in other branches of technology. The wide transparent bandwidth of $In_2O_3$ films makes it a good candidate as a waveguide material. By varying the mole percentage of $In_2O_3$, the index of refraction and the band gap of the $In_2O_3$:Sn can be manipulated over a wide range of interest. The index of refraction of an indium tin oxide film can be represented by


0-8194-0714-3/91/$4.00

$$n^2 = \varepsilon_{opt} - \frac{4\pi Ne^2}{m^* \omega_o^2} \qquad (1)$$

where $\varepsilon_{opt}$ is the high-frequency permittivity and $\omega_o$ is the frequency of electromagnetic oscillations at which measurements were carried out ($\omega_o = 2\pi c/\lambda$). The decrease in the index of refraction (Figure 1) with the decrease in the $In_2O_3$ mole percentage implies that the carrier concentration is increased as more $SnO_2$ is doped into the $In_2O_3$ film. The experimental values of the energy band gap, graphed in Figure 2, were obtained by detecting the absorption edge.

The band gap varies from 3.1 eV (0.4 μm) with pure $In_2O_3$ to ~ 3.7 eV (0.335 μm) with 5% $SnO_2$ in the $In_2O_3$ film. For all optical modulation (to be described in Section 4.0), the band gap energy $E_g$ is an important parameter in determining the wavelength of optical activation. To date, there is no reported data on the band structure of indium tin oxide film. The result shown in Figure 2 is correct for both direct and indirect band gaps. In the case of indirect band gap absorption, a phonon must be absorbed to supply the missing crystal momentum. This is typically a few hundredths of an electron volt and therefore of little consequence except in semiconductors with a very small energy gap.[4]

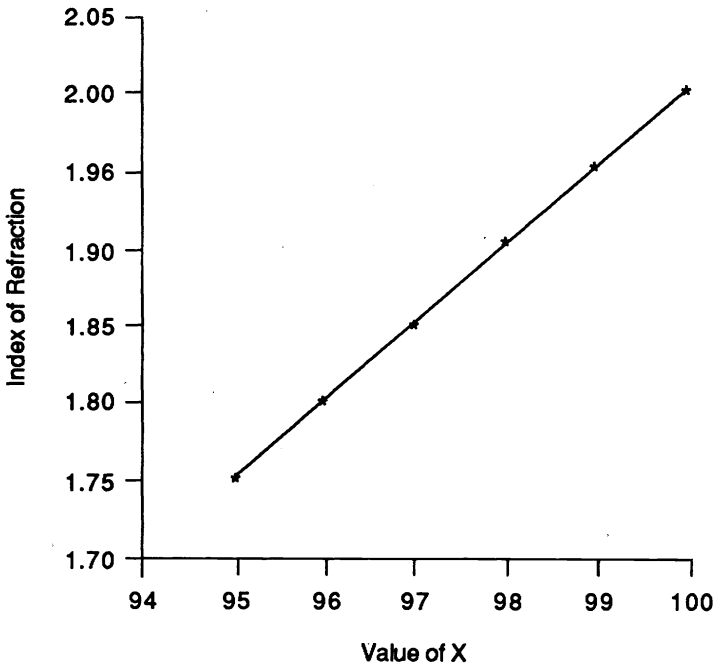


Figure 1 Index of refraction of $In_2O_3$:Sn film at 632.8 nm wavelength. X represents the pole percentage of $In_2O_3$.

## 2.1 Waveguide characteristics

A variety of $In_2O_3$:Sn guided wave devices working in the single-mode regime was investigated. Formation of a single-mode waveguide was first confirmed by using prism coupling methods. With a 98%, 300 nm $In_2O_3$:Sn film, a single-mode TM (transverse magnetic) waveguide was experimentally confirmed. The result of the demonstration is displayed in Figure 3(a) where a bright streak is apparent in the photograph.

The measured effective index was 1.750, very close to the theoretical result ($In_2O_3$:Sn (n = 1.9) on glass (n = 1.51) has an effective index value of 1.770). The mode dot coupled out of the output prism is further illustrated in Figure 3(b). The observation of an m-dot rather than an m-line insures the waveguide quality. Note that the smoothness of the glass substrate plays an important role for the realization of such a waveguide. To further characterize the waveguide propagation loss, loss measurement was conducted using a two-prism method. Both TE and TM modes were measured. The waveguide propagation losses of 3 dB/cm and 8 dB/cm shown in Figure 4 were experimentally confirmed for TM and TE, respectively. The measured results implied that a TM guided wave is more suitable than a TE guided wave for making a modulator with high modulation depth.

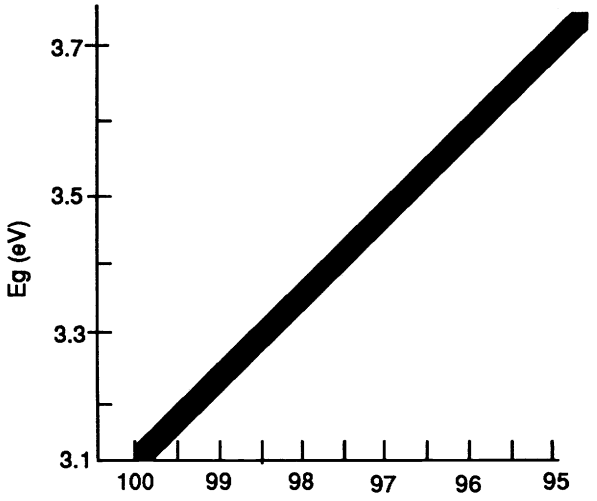


Figure 2 Energy gap of $In_2O_3$:Sn film as a function of the $In_2O_3$ mole percentage (%)

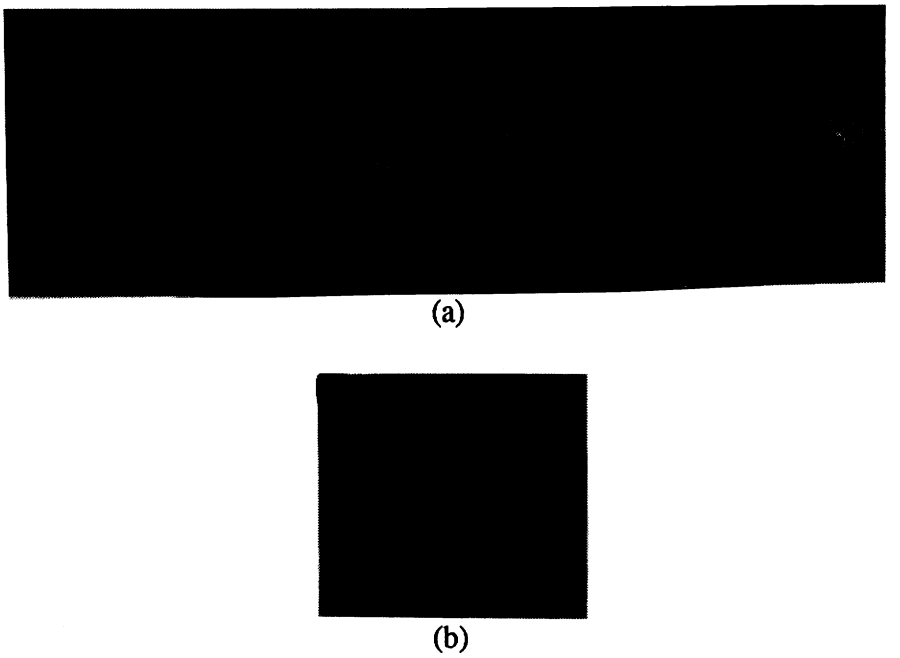


Figure 3 (a) Single-mode $In_2O_3$:Sn waveguide on glass substrate (the total length of the waveguide is 5 cm). (b) Mode dot coupled out of a prism coupler

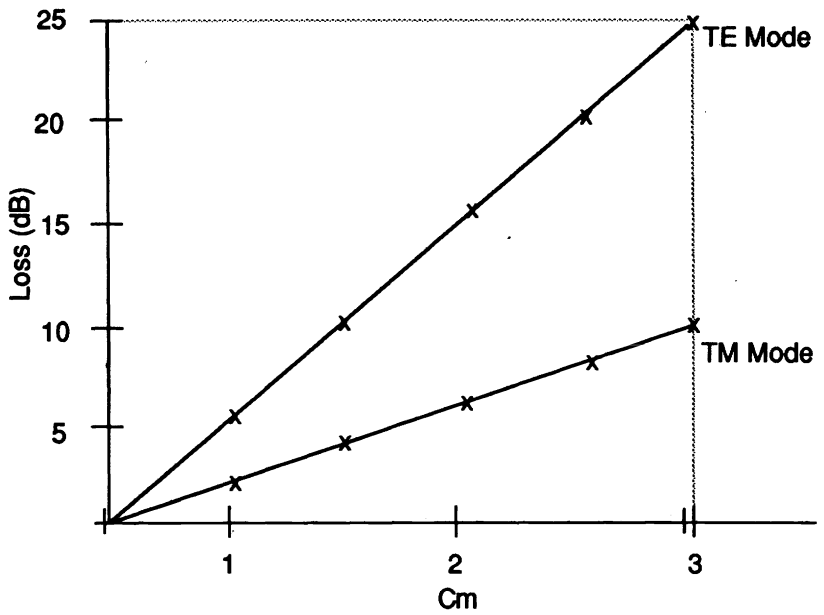


Figure 4 Loss measurement of single-mode indium tin oxide waveguide on glass substrate (98% $In_2O_3$ mole concentration)

## 3.0 WORKING PRINCIPLE OF THE DEVICE

The electrooptic and all optic modulation of the indium tin oxide film was carried out by manipulating the carrier concentration of the $In_2O_3$:Sn. There are two methods to provide this manipulation. The first method is to electrically inject a time-varying current and the second is to optically activate the device using a short wavelength light source with photon energy larger than the band gap energy $E_g$. For either case, the carrier concentration of the indium tin oxide film will be perturbed and an index modulation within the film will be generated accordingly.

A very large current induced index change was reported on Si, GaAs-GaAlAs and InGaAsP-InP.[5,6] Because a current induced index change is much stronger than the linear electrooptic effect, we can make an active device by injecting a time dependent carrier concentration. When the optical signal carrier to be modulated is coupled to the single-mode waveguide, the induced current will interact with the guided wave. The equation of motion of an electron in an electric field $E_y$ of frequency $\omega_o / 2\pi$ along the vector direction of the electric field, say y, is

$$m_e^* \frac{dv_y}{dt} = -e \cdot E_y = -e \cdot E \cdot e^{i\omega_o t} \tag{2}$$

where $m_e^*$ is the effective mass of an electron and $E_y$ is the electric field. The solution for Eq. (2) is

$$V_y = V_{y_o} + \frac{ie \cdot E}{\omega \cdot m_e^*} e^{i\omega_o t} \tag{3}$$

Because the mean velocity without the influence of $E_y$ is 0, the first term $V_{y_o}$ will be zero also. The current induced by this optical field is

$$J_y = N \cdot e \cdot V_y = \frac{iN \cdot e^2 \cdot E}{\omega \cdot m_e^*} e^{i\omega_o t} \tag{4}$$

The current density induced by an electric field can also be written as

$$J_y = \sigma \cdot E_y \tag{5}$$

where $\sigma$ is the conductivity. Comparing Eqs. (4) and (5), we have

$$\sigma = \frac{iN \cdot e^2}{\omega \cdot m_e^*} \tag{6}$$

The dielectric constant and conductivity enter into the determination of the optical properties of a solid only in the combination [4]

$$\varepsilon(\omega) = n_o^2 + \frac{4\pi i\sigma(\omega)}{\omega} \tag{7}$$

where $n_o$ is the index of refraction without the influence of current. From Eq. (6), we can easily write Eq. (7) in the following form:

$$n = (\varepsilon)^{1/2} \sim n_o \cdot \left(1 - \frac{2\pi N e^2}{m_e^* \, \omega^2 n_o^2}\right) \tag{8}$$

The $\Delta n$ value in this condition is

$$\Delta n = \frac{-2\pi N e^2}{m_e^* \, \omega^2 n_o} \tag{9}$$

Because both electrons and holes contribute to the current, Eq. (9) is written as

$$\Delta n = \frac{-2\pi N_e e^2}{m_e^* \, \omega^2 n_o} + \frac{-2\pi N_p e^2}{m_p^* \omega^2 n_o} \tag{10}$$

An index modulation on the order of $10^{-2}$, which is two orders of magnitude higher than the linear electrooptic effect, has been reported for current induced index modulation.[1,2]

The device structure we employed is a Fabry-Perot waveguide resonator. The reflection mirrors are constructed using a holographic phase grating (HPG). The existence of the waveguide propagation loss and less than 100% reflectivity of the HPG reduce the peak transmission to less than unity. Figure 5 shows the curves of $I_t/I_i$ with propagation loss as a parameter 30% reflectivity of the holographic mirrors is assumed in this calculation. The structure of the basic device fabricated is shown in Figure 6. The grating fringe associated with the holographic mirrors is evident. The index modulation within the cavity can be generated either by current injection or by optical activation.

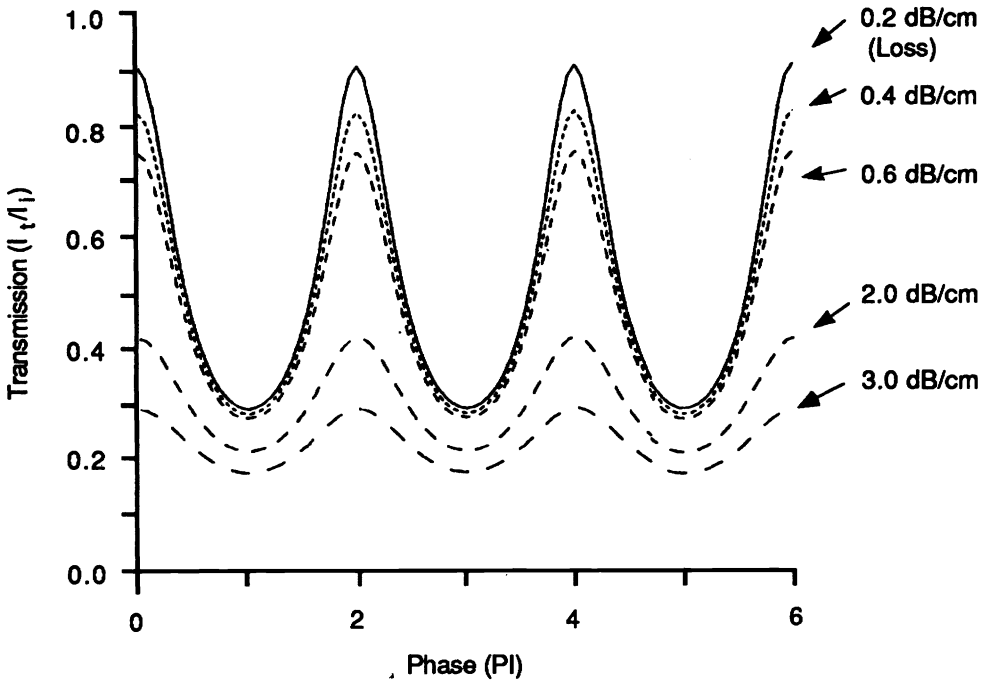


Figure 5 Transmission ($I_t/I_i$) of a Fabry-Perot waveguide modulator as a function of the phase shift with waveguide propagation loss as a parameter.

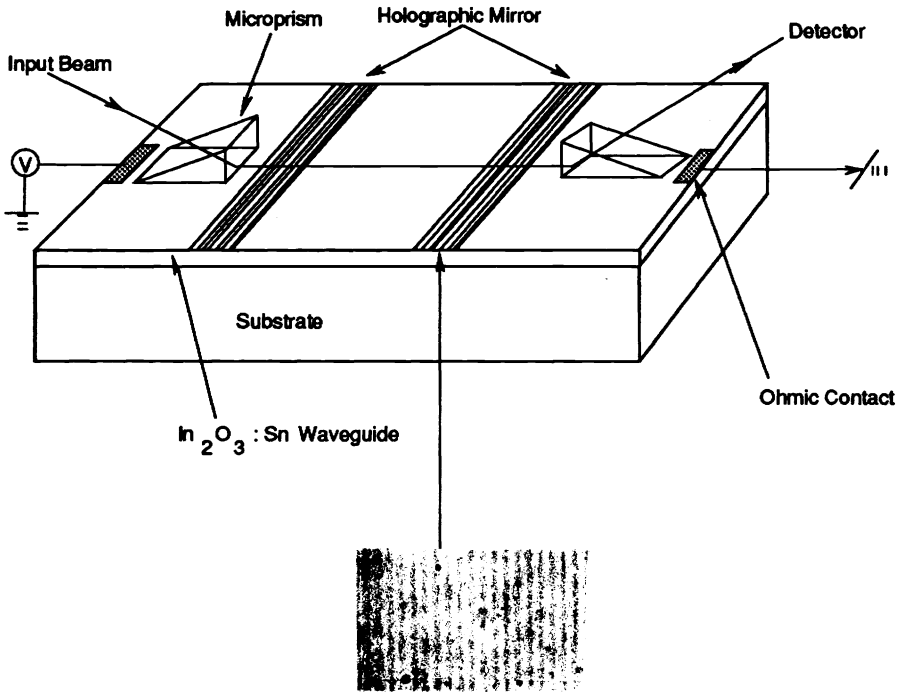


Figure 6 Device structure for an $In_2O_3$:Sn waveguide modulator

## 4.0 EXPERIMENTAL RESULTS

### 4.1 Current induced modulation

An indium tin oxide waveguide modulator using the current injection method was demonstrated first. The setup for waveguide coupling and current injection is shown in Figures 7 and 8. The phase-matching angle for prism coupling is achieved by changing the azimuthal angle of the stage such that

$$N_{eff} = N_p \cos \theta_c \tag{11}$$

can be achieved. In Eq. (11), $N_{eff}$ is the effective index and $N_p$ and $\theta_c$ are the prism index and the prism coupling angle (within the prism), respectively. The current injection was realized by applying an AC voltage across the two ohmic contacts shown in Figure 6. Figure 8 is a close-up view of the $In_2O_3$:Sn waveguide device. Ohmic contacts, input and output prism couplers and the waveguide substrate are within the view of this photograph. A modulation depth of 18% is observed at an AC pulse signal of 60 kHz and an amplitude of 15 volts.

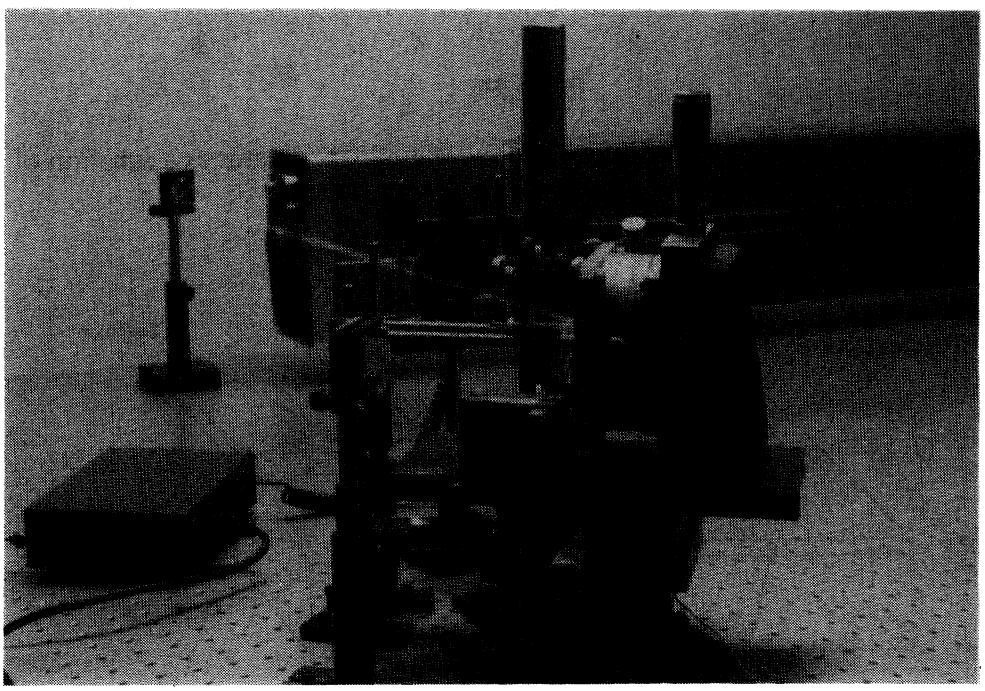

Figure 7 Setup for current induced modulation on $In_2O_3$:Sn thin film.

Note that the 18% modulation depth shown in Figure 9 is directly measured through the reference signal, which has 100% modulation depth. The measured index modulation due to current injection was on the order of $10^{-3}$. Note that the modulation depth is limited by 1) the waveguide propagation loss which is 3 dB/cm for TM mode and 2) the reflectivity of the holographic mirror which is ~ 30% in our experiment. Note that a modulation depth close to 100% can be realized by minimizing the waveguide propagation loss and by enhancing the reflectivity R of the holographic mirrors. A further current induced modulation was demonstrated by injecting an electrical current into the indium tin oxide film through the ohmic contact. The $In_2O_3$:Sn waveguide has a waveguide effective index very close to cutoff ($N_{eff}$ = 1.525). Unlike the

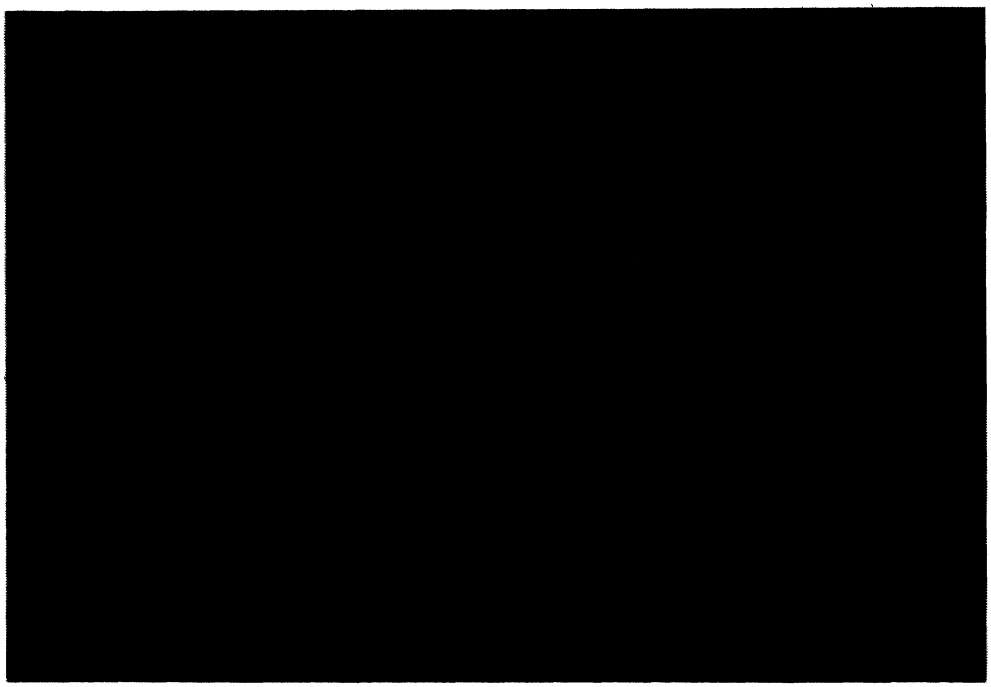

Figure 8 Current injection through the ohmic contact. Prism couplers are clearly shown.

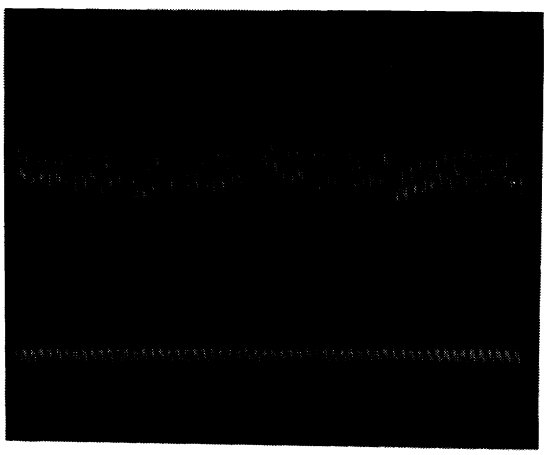

Figure 9 Detected signal (60 kHz) with 18% modulation depth. Reference signal with 100% modulation depth is also indicated.

linear electrooptic effect where the index modulation is electric-field orientation dependent, the current induced index modulation reduces the index modulation regardless of the direction of current injection. Consequently, the cutoff modulation can be realized by injecting a current into a single mode $In_2O_3$:Sn waveguide having an effective index close to the cutoff boundary. The voltage needed to achieve the cutoff modulation is [8]

$$V = \frac{(N_{eff} - N_s) \cdot R}{k} \qquad (12)$$

where k is a constant representing the linear response of the refractive index of the film, R is the resistance of the film, and $N_S$ is the substrate index of the waveguide. Figure 10 shows the experimental throughput of an acousto-optically modulated HeNe signal (85 MHz) under a DC voltage of 0, 20, and 30 volts applied to the ohmic contact associated with the device (Figure 6). An extinction ratio of 26 dB was experimentally confirmed in this case. From the results shown in Figure 10, one can conclude that indium tin oxide film can be used as a power limiter.

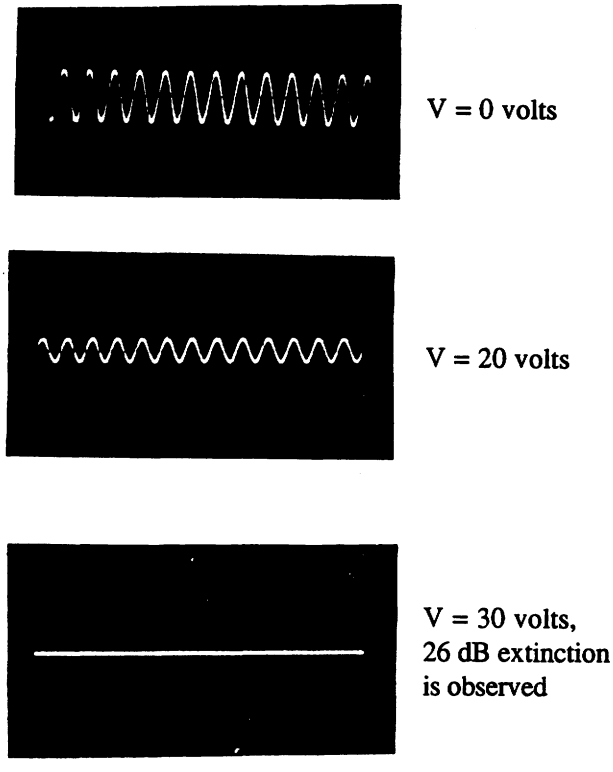


Figure 10 Throughput intensity modulation of acoustooptically modulated HeNe light (85 MHz) using DC power of (a) 0 volt, (b) 20 volts, and (c) 30 volts.

## 4.2 All-optical modulation

Based on the principle described in Section 3.0, an alternative to activating the $In_2O_3$:Sn waveguide modulator is to generate a time-dependent carrier density through electron-hole pair generation. The band gap energy varies from 3.1 eV to 3.7 eV (Figure 2) which corresponds to an optical wavelength between 0.4 to 0.335 μm. To investigate the possibility of absorption due to shallow-level and deep-level states,[7] an Argon laser working at 436 nm was first employed for the demonstration. The experimental setup is shown in Figure 11 where HeNe 632.8 nm light is prism coupled into the indium tin oxide planar waveguide. The 436 nm is focused into the active region between the two holographic mirrors (Figure 6). The waveguide device used for this demonstration is the same as that of the current-induced modulator introduced in Section 4.1. A 436 nm light with intensity as high as 5 W/mm$^2$ was shone on the active region. Experimentally, no intensity modulation was observed under this condition. This result implies that the absorption due to

deep and shallow-levels is negligible. For our experimental scheme, index modulations as small as $10^{-6}$ allow us to clearly observe the phenomenon. By shifting the activation light source from 436 nm to 355 nm (third harmonic of the YAG laser), an all-optical experiment was conducted. 50 mW, 355 nm UV light was generated from the BBO crystal. By collimating and imaging the UV light onto the active region through UV lenses, electron-hole pairs can be generated from the indium tin oxide film (98% $In_2O_3$). The setup used to facilitate the demonstration is shown in Figure 12 where a label is attached to each individual instrument. A YAG laser, a third harmonics generator (BBO cavity), a UV beam chopper, a HeNe laser, prism couplers, an $In_2O_3$:Sn waveguide modulator, a Si detector and electronic equipment for amplification and detection are clearly indicated. The purpose of the beam chopper is to modulate the UV light so that a time-dependent carrier concentration can be created within the indium tin oxide film. The throughput light or HeNe guided wave is imaged onto a p-i-n silicon detector which is connected to an amplifier. The outcome of the detected signal is displayed in Figure 13. A 4 kHz modulated guided wave which is synchronized with the electrically chopped UV light at 632.8 nm is present. The modulation depth of the signal was measured to be ~ 15%. The modulation speed is limited by the chopper frequency which has a maximum of 4 kHz.

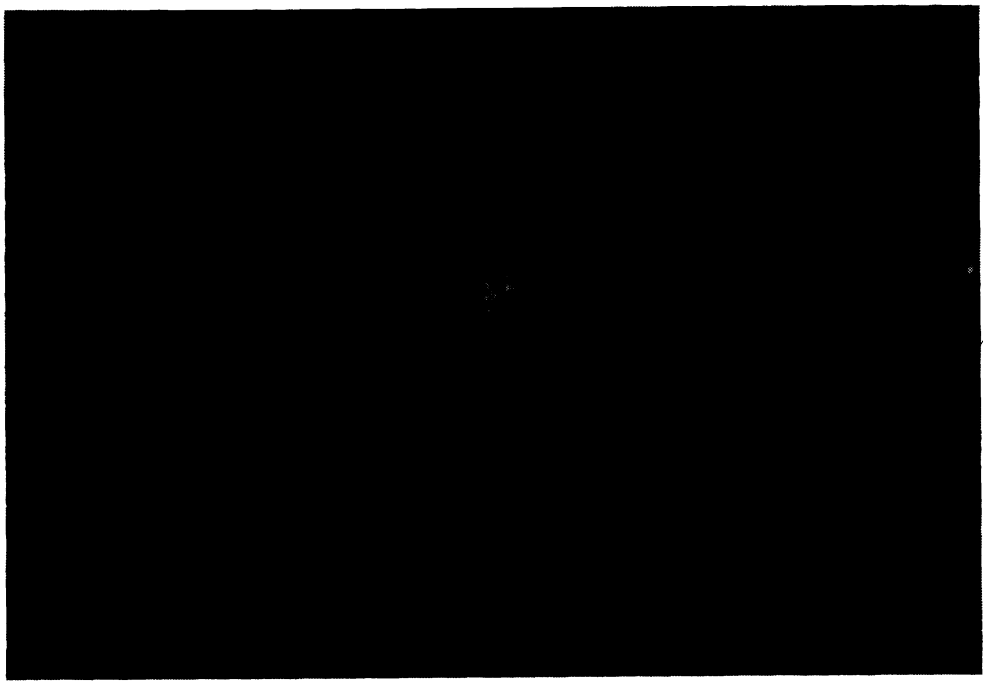

Figure 11 Experimental setup of all optical modulation using 632.8 nm HeNe as the signal carrier beam and 436 nm argon laser as the activation source.

## 5.0 FURTHER APPLICATIONS

An indium tin oxide waveguide modulator is introduced for the first time. Implementation of either current or UV optical activation source on the device is a straightforward method to realize such a device. Manipulation of the band gap by changing the ratio of $In_2O_3$ and $SnO_2$ is a promising approach for microstructure optoelectronic devices. An array of applications are feasible based on the present technology. These include current sensors, ozone UV sensors, phase resonant ATR modulators, power limiters, phased array antennae, and multi-quantum well (MQW) devices. A detailed description of each individual application can be found in Ref. 9.

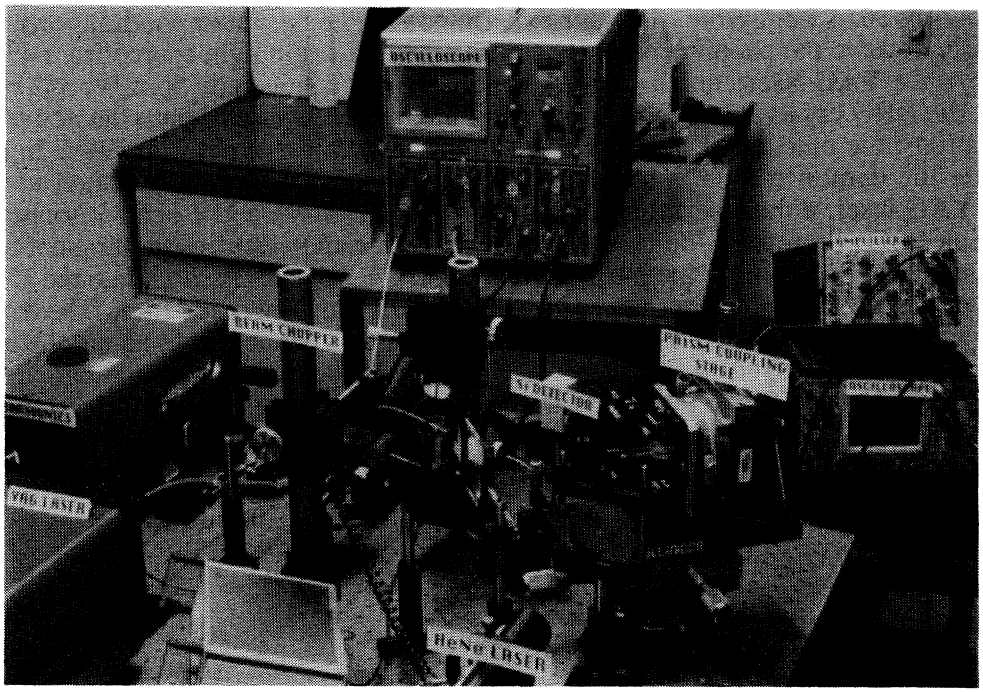

Figure 12 Experimental setup of all optical modulation using 632.8 nm HeNe as the signal carrier beam and 355 nm laser light as the activation source.

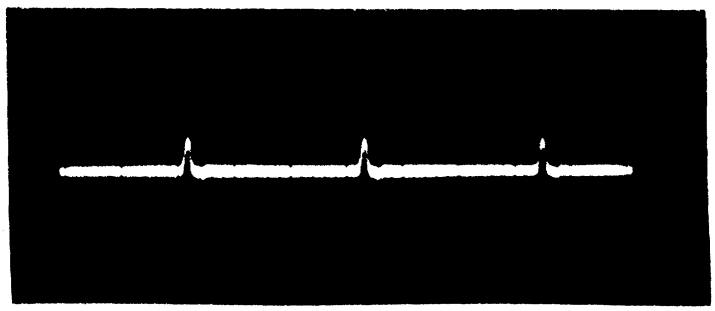

Figure 13 4 kHz modulated signal of 632.8 nm HeNe guided wave using 355 nm UV laser as the activation source. Modulation depth of 15% is observed.

The feasibility of engineering the band gap by altering the concentration ratio of $In_2O_3$ and $SnO_2$ provides us with a far-reaching application scenario--MQW. Figure 14 is a schematic of the $In_2O_3$:Sn compositional superlattices which asssume a direct band gap. It is clear that both nonlinear all-optical devices such as optical bistable devices [10] and the electro-absorption devices such as self electrooptic effect devices (SEED) [11] are very attractive.

## 6.0 CONCLUSIONS

We have successfully demonstrated a cost-effective way of generating an indium tin oxide semiconductor film which was proven to be an acceptable waveguide for both TE and TM modes. The band gap and thus

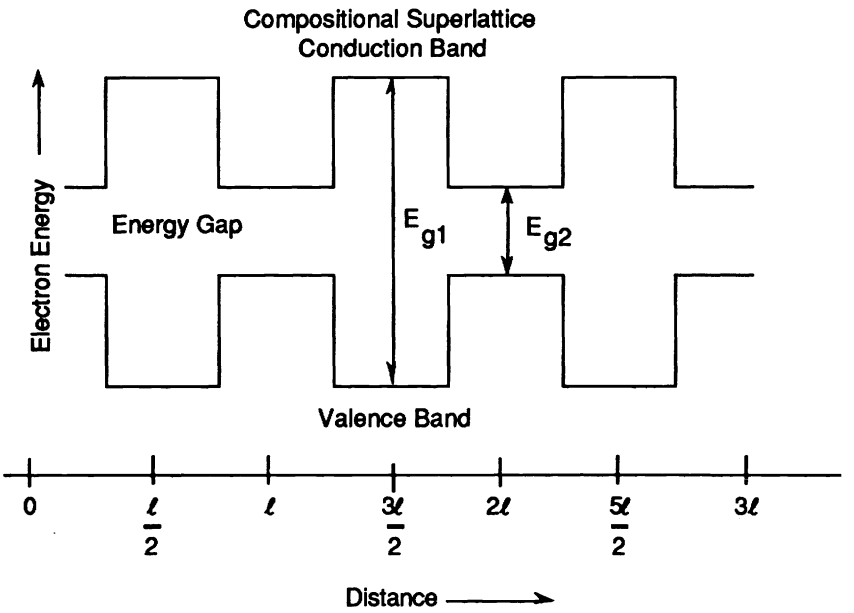


Figure 14 Multi-quantum well structure by altering $In_2O_3$ and $SnO_3$ concentration.

the activation photon energy can be tuned from 3.1 eV (0.4 μm) to 3.7 eV (0.335 μm) by changing the ratio of $In_2O_3$ and $SnO_2$. Phase modulation using an $In_2O_3$:Sn single-mode waveguide in conjunction with two holographic mirrors was demonstrated in both a current injection scheme and an optical activation scheme. The 18% modulation depth for current injection modulation at a pulse frequency of 60 kHz and all-optical modulation with 15% modulation depth using 355 nm light (third harmonic of the YAG laser) were experimentally confirmed. The relatively low modulation depth was attributed to the low reflectivity of the holographic mirrors and 3 dB waveguide propagation loss. A further experiment on an indium tin oxide waveguide modulator working in the cutoff regime was conducted by injecting a DC current into the waveguide through the associated ohmic contact. Modulation depths as high as 26 dB were measured. Due to the simplicity and innovativeness of the proposed concept, a number of highly feasible applications were presented. These include current sensors, UV sensors for the ozone shell, short interaction length ATR waveguide modulators, phased-array delay lines and multi-quantum well devices. Table 1 summarizes the indium tin oxide waveguide devices and compares them with existing external EO modulators. It is clear that the proposed $In_2O_3$:Sn waveguide modulator has advantages in parameters 3, 4, 5, 6, 8, 9, 10, and 11. For parameters 1, 2, and 5, the proposed waveguide modulator is equivalent to the existing devices. The major uncertainty is the modulation speed of such a device. The mechanism of introducing an index modulation within the semiconductor film is to perturb the minority carrier concentration of the film. Therefore, the element determining the switching speed will be the carrier lifetime of the electron-hole pairs.

This research program was sponsored by the National Science Foundation .

## 7.0 REFERENCES

1. R. A. Soref and B. R. Bennett, "Electro-Optic Effects in Silicon," *IEEE J. of Quantum Electron.*, vol. QE-23, p. 123 (1987).
2. J. P. Lorenzo and R. A. Soref, "1.3 mm Electro-Optic Silicon Switch," *Appl. Phys. Lett.*, vol. 51, p. 6 (1987).

Table 1. Demonstrated Features of the $In_2O_3$:Sn Waveguide Modulator Compared With Those of Existing Active Devices

| | Technology / Parameter | $In_2O_3$:Sn | $LiNbO_3$ E-O Device | GaAs E-O Device | MQW | Plasmon Modulator | $\chi^{(3)}$ Nonlinear All-Optical Device |
|---|---|---|---|---|---|---|---|
| 1 | Signal Carrier Bandwidth | Visible and Near IR | Visible and Near IR | IR | Very Low | Extremely Low | Low |
| 2 | Power Consumption | 1W | 1W | 1W | 10 mW | 1W | 1 MW |
| 3 | Status of Development | New Concept | Well Developed | Well Developed | Well Developed | Recently Developed | Recently Developed |
| 4 | Refractive Index Modulation | $\sim 10^{-3}$ | $\sim 10^{-4}$ | $\sim 10^{-4}$ | $\sim 10^{-3}$ | $\sim 10^{-4}$ | $\sim 10^{-4}$ - $10^{-5}$ |
| 5 | Extinction Ratio | ≥ 30 dB | ≥ 30 dB | ≥ 30 dB | ≥ 30 dB | ≥ 20 dB | ≥ 40 dB |
| 6 | Interaction Length | 100 μm[c] to 1 cm | ~5 mm | ~ 5 mm | S~ 10-100 μm | ~ 100 μm | 1 mm to 1 cm |
| 7 | Modulator Speed | ?[b] | 30 GHz | 50 GHz | ~ 10 GHz | 100 GHz[d] | 20 GHz |
| 8 | Reliability | Very Good | Good | Good | Poor | Poor | Poor |
| 9 | Cost | Low | High | High | Very High[d] | High | Very High[e] |
| 10 | Practicality | Very Good | Good | Good | Poor | Poor | Poor |
| 11 | Coherence of Signal Carrier | Not Required[f] | Required | Required | Required | Required | Required |

[a] 5 mm interaction length was demonstrated in Phase I.
[b] Only limited by carrier lifetime, no experimental result has been demonstrated so far on high speed modulation.
[c] Current injection scheme needs longer length (~1 cm), all optical modulator need only ~100 μm interaction length.
[d] Theoretical prediction to 100 GHz. No experimental results are available on high speed modulation.
[e] Needs high power laser as the activation source.
[f] Both LEDs and LDs can be employed for the device working in the cutoff regime.


3. J. Manning, R. Olshansky, and C. B. Su, "Strong Influence of Nonlinear Gain on Spectral and Dynamic Characteristics of InGaAsP Laser", *Electron. Lett.*, vol. 21, p. 496 (1985).
4. N. W. Ashcroft et al., Solid State Physics, (Ithaca, NY, Cornell University, 1976).
5. N. K. Dutta, N. A. Olsson, and W. T. Tsang, "Carrier Induced Refractive Index Change in AlGaAs Quantum Well Lasers," *Appl. Phys. Lett.*, vol. 45, p. 836 (1984).
6. K. Tada and Y. Okada, "Bipolar Transistor Carrier-Injected Optical Modulator/Switch: Proposal and Analysis," *IEEE Electron. Device Lett.*, vol. EDL-7, p. 605 (1986).
7. S. M. Sze, Physics of Semiconductor Devices (Hohn Wiley & Son, Inc., 1983).
8. R. T. Chen et al., "Thermally Annealed Single-Mode Proton-Exchanged Channel Waveguide Cutoff Modulator," *Opt. Lett.*, vol. 11, p. 546 (1986).
9. R. T. Chen, "Polarization Sensitive Electrooptic and All-Optical $In_2O_3$:Sn Waveguide Modulator," Final Report to NSF, Contract No. ISI-9061016 (1991).
10. Y. Arakawa and H. Sakaki, "Multiquantum Well Laser and its Temperature Dependence of the Threshold Current," *Appl. Phys. Lett.*, vol. 40, p. 939-941 (1982).
11. D. A. B. Miller, D. S. Chemla, T. C. Damen, T. H. Wood, C. A. Burrus, Jr., A. C. Gossard, and W. Wiegmann, "The Quantum Well Self-Electrooptic Effect Device: Optoelectronic Bistability and Oscillation and Self-Linearized Modulation," *IEEE J. Quantum Electron.*, vol. 21, no. 9, p. 1492 (1985).